# INVESTIGATION OF GRAPHENE NANOSHEETS REINFORCED ALUMINUM MATRIX COMPOSITES

X. M. DU*, R. Q. CHEN, F. G. LIU
*School of Materials Science and Engineering, Shenyang Ligong University, Shenyang 110159, China*

Aluminum matrix composites strengthened with graphene sheets (Al-Gr) were fabricated by the combination of powder metallurgy and rolling methods. The morphologies and structures of Al-Gr powders as ball-milled were studied for different time. The effects of the graphene sheets content on the microstructures, density and wear property of the composites were also investigated. It is indicated that the graphene sheets are gradually dispersed into the aluminum matrix with increasing the ball-milling time and a uniform dispersion is achieved after ball-milling for 24 h. And no obvious agglomeration of graphene is observed in as-sintered and as-rolled composites for the contents of graphene sheets up to 1.0 wt.%. The coordinated deformation of multilayer graphene sheets occurs with the deformation of the surface grains during rolling, which may cause a significant reduction in the number of layers of graphene sheets. With increasing the graphene sheets contents, the density of the Al-Gr composites shows an decrease. The maximal hardness of Al-Gr composites were 89.3 ± 3.2 HV at 0.7 wt.% of graphene content, showing 39.5% increments over pure aluminum. The coefficient of friction and wear rate in Al-Gr composites are significantly reduced compared with those in the matrix.

(Received October 22, 2016; Accepted January 14, 2017)

*Keywords*: Aluminum matrix composites, Graphene sheets, Powder metallurgy

## 1. Introduction

Successful isolation of the graphite monolayer, graphene, in 2004 has opened up a new field of research [1,2], and has attracted much attention as a fascinating candidate for nanoelectronics and spintronics [3-6] due to its excellent properties. In addition, higher strength and toughness are also the potential advantage of graphene in engineering application. In 2008, researchers conducted the first strength test on graphene and published the results [7]. The studies found that the intrinsic strength of the material was 130 GPa. These researches establish graphene as the strongest material ever measured some 200 times stronger than structural steel. Subsequent experimental study has confirmed this result [8].

Graphene is by far the thinnest and the toughest material. How to improve the strength and toughness of the composites by using graphene has become a widely concerned issue. At present, research results on nanoscale graphene-reinforced polymer [9] and ceramics [10] matrix composites have been reported. The tensile strength of Polyvinyl alcohol (PVA) filled with 0.7 wt.% graphene nanosheets increased 76% [9]. The bending strength and breaking strength of $Al_2O_3$ ceramic matrix filled with 0.78% volume fraction of graphene nanosheets increased 30.75% and 27.20%, respectively [10]. However, there is few report on the graphene reinforced-metal matrix composites. How are graphene nanosheets evenly dispersed in the metal matrix. How do good contact interfaces form between graphene nanosheets and metal matrix.

*Corresponding author. du511@163.com

And how does the microstructure of graphene nanosheets remain in composites. Solving these problems is still a big challenge.

In this study, Al-Gr composites were fabricated by using vacuum hot pressing and rolling methods. And then their microstructure and mechanical properties were measured. The mechanism of reinforcement of the graphene sheets is also discussed.

## 2. Experimental details

### 2.1 Materials

Graphene sheets used in our experiments were prepared by modified hummers method as reported previously [11]. The experimental material is natural graphite with particle size of about 45 um. Natural graphite was reduced at 95 ℃ for 24 hours by using hydrazine hydrate. Graphene sheets with the thickness of several atomic layers were obtained. The preparation method was similar to that of Ref. [11]. Atomized pure aluminum powder (AnShan Steel Industrial Fine Aluminum, Inc., Liaoning, China) with an average size of 20 um and chemical composition (Fe 0.071 wt.%, Si 0.067 wt.%, Cu 0.002 wt.%) was used as matrix material.

### 2.2 Preparation and characterization of Al-Gr composites

Pure aluminum powders were initially mixed with 0.3, 0.7, 1.0, 1.2 wt.% as-prepared graphene sheets in a conventional rotating ball milling machine using the stainless jar and balls. Ball milling was carried out in argon atmosphere at a rotating speed of 90 rpm for 1-96 h with ball-to-powder weight ratio of 3:1. The above prepared Al-Gr powders were loaded into a graphite die with a diameter of 50 mm. A sheet of graphitic paper was placed between the punch and the powders as well as between the die and the powders for easy removal. The compact Al-Gr composite billets were vacuum hot pressed at 605 ℃ for 1.5 hours under a pressure of 25 MPa by powder metallurgy. The Al-Gr composites were prepared, and followed by warm rolling at 520 ℃ with thickness reduction of 20-30% one pass. For comparison, a pure Al sample was also fabricated under the same conditions.

Microstructures of as-hot pressed and as-rolled composites were observed with X-ray diffractometer of Rigaku Ultima IV with Cu Ka radiation. The surface morphology was observed by a scanning electron microscopy (SEM) of S-3400N and an optical microscope of Carl Zeiss Axioert200MAT. Density was measured by the Archimedes method. Hardness measurements of composite samples were carried out on a Vickers hardness testing machine (Shanghai Shuangxu, Inc., HVS-50, China), using a load of 9.8 N, and the mean values of at least five measurements conducted on different areas of each sample was considered.

Dry sliding wear tests were carried out on the composites at ambient laboratory conditions by a universal friction and wear testing machine (Jinan Jingcheng, Inc., MMW-1A, China). The test material in the form of pins of diameter 16 mm and height 10 mm were slid against a rotating steel ring (counter face) with a hardness of 62 HRC, having the diameter of 32 mm and thickness of 10 mm. Specimens were subjected to an initial run-in period until the whole surface of the pin was in full contact with the ring surface. They were then ground with 800 grit silicon carbide paper, cleaned in an ultrasonic bath with acetone for 6 min and hot wind dried below 100 ℃. Wear tests were undertaken under the normal load of 50N, the rotating speed of steel ring of 60 r/min and the test time of 10 minutes. The mass of each specimen was measured before and after each wear test and the mass difference was then converted to volumetric wear rates using the measured density of each material and the total sliding distance. Friction coefficient measurements were made using a transducer to measure the deflection of the pin holder caused by the ring rotation. The system was calibrated by applying known tangential loads and noting pin deflections.

## 3. Results and discussion

### 3.1 Microstructure characterization

Typical microstructures of pure aluminum powder and graphene observed by SEM are shown in Fig. 1. The particle shape of aluminum is regularly spheroidal. The mean size of the particles appears to be ～20um with some smaller particles of 3-4 um and some larger particles of about 20 um (Fig.1 (a)). Graphene sheets showing a feather like, translucent, show that the thickness is very thin. The radial size is in micron order. And they have the typical characteristics of the folded structure (Fig.1 (b)). Fig. 2 shows X-ray diffraction pattern of graphene sheets. There exists a boarding diffraction peak located near 26°, indicating that graphene sheets are very small. This agrees with the reported results in Ref. [12].

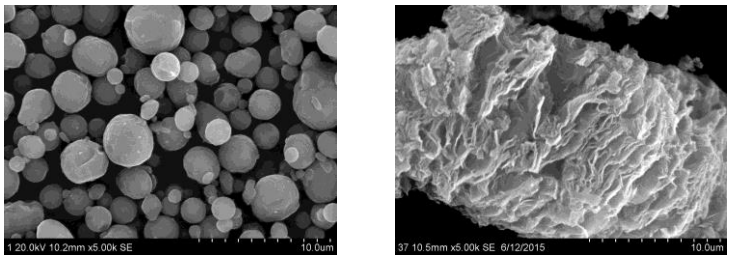


(a) (b)

*Fig. 1. SEM micrograph of powders used, (a) pure aluminum powder, (b) Graphene.*

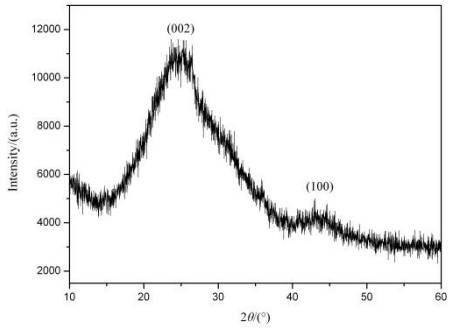


*Fig. 2. X-ray diffraction pattern of grapheme*

Milling time and graphene content have an important influence over morphology, powder size, microstructure and physical properties in Al-Gr composites. Fig. 3 and Fig. 4 show a comparative analysis for different samples with different milling time and graphene content. Fig. 3 presents the morphology evolution of Al-Gr composite powders during the milling process as a function of milling time. A visible plastic deformation is observed in several particles, which present a flake-like morphology, in samples beyond 1 h of milling (Fig. 3 (b) – (d)). During ball milling, plastic deformation of raw metals is repeated and the metals mix by collisions of the surfaces of moving balls and a rotating milling pot. An increase in particle size from 1 h to 96 h of milling time is observed, as a consequence of the increase in the number of impacts of particles by the milling media, which indicates a predominance of the cold welding over the fracture stage during milling process. It is important to notice that clusters of graphene sheets are not visible for various milling time. It indicates an excellent dispersion of the graphene in the aluminum matrix in short periods of milling time by ball-milling method. Longer milling times have no obvious improvement for the dispersion of graphene sheets in aluminum matrix. The ball milling time is determined to be 24 hours in this experiment.

The effect of graphene content on it's dispersion is shown in Fig. 4. It can be seen from the figure that the graphene content is so low that a small amount of graphene sheets are observed (Fig. 4 (a)). With the increase of the graphene content, the graphene sheets on the aluminum particles gradually increased, which mainly distributed on the surface of the aluminum powders, and show no obvious agglomeration of graphene sheets when the content of graphene in the Al-Gr composites is up to 1 wt%. However, the agglomeration of graphene sheets was observed in Al-Gr composite with the content of graphene up to 1.2 wt% (as shown in Fig. 4 (d)).

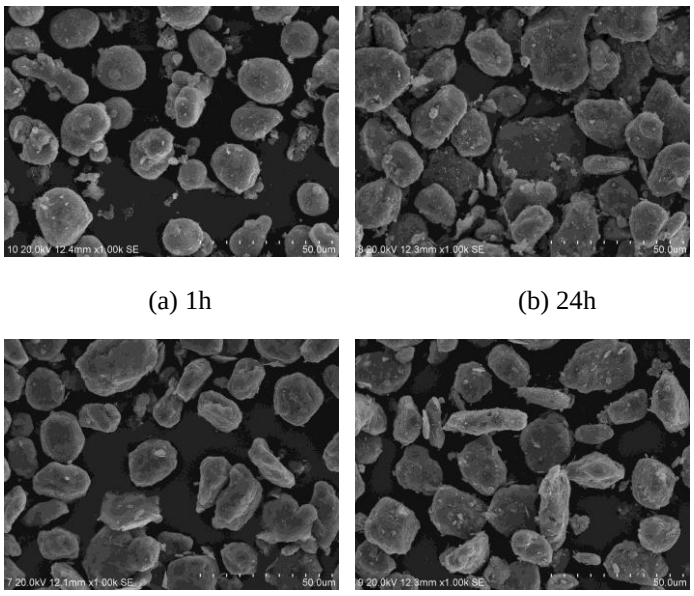

(a) 1h (b) 24h

(c) 72h (d) 96h

*Fig. 3 SEM for Al- 1.0 wt% Gr composite for 1, 24, 72 and 96 h of milling time in the as-milled condition.*

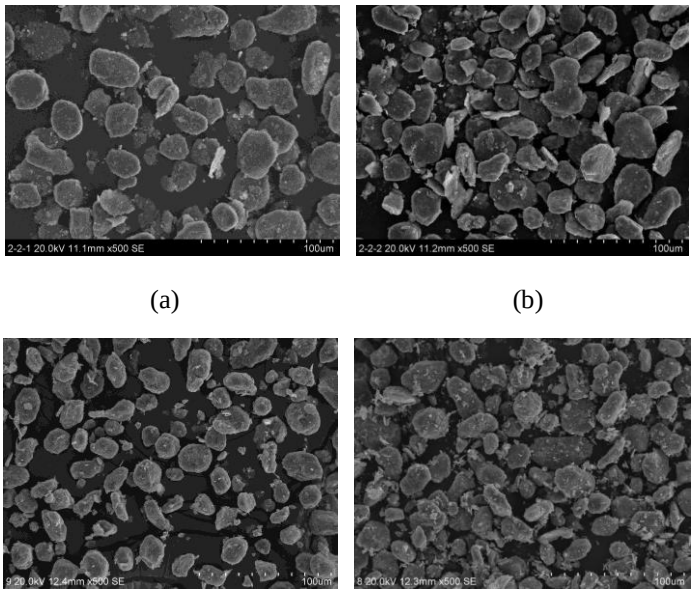

(a) (b)

(c) (d)

*Fig.4 SEM micrographs of the mixtrue of aluminum powder particles and graphene sheets with different content at 24 h, (a) 0.3 wt.%, (b) 0.7 wt.%, (c) 1.0 wt.%, (d) 1.2 wt.%.*

X-ray diffraction patterns from the pure aluminum and it's composites in hot-pressed condition are presented in Fig. 5. All samples have major aluminum peaks at 38.8° (1 1 1), 45.0° (2 0 0), 65.4° (2 2 0), 78.5° (3 1 1) and 82.7° (2 2 2). However, reflections attained to the carbon element were not presented for any of the samples. This is attributed to the nanometric size and the low content of the reinforcement phase, which can not be detected due to the detection limit presented by XRD for second phases [13].

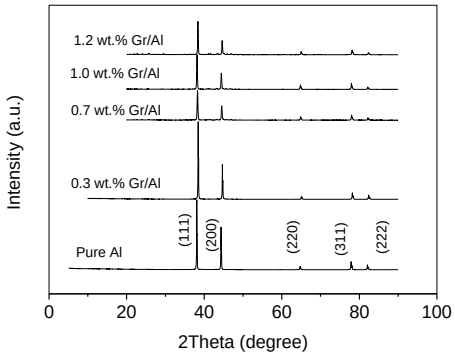


*Fig. 5. XRD patterns of pure Al and various Al-Gr composites*

The optical photographs of cross-sections of the hot-pressed Al-Gr composites with different graphene contents are shown in Fig. 6. It can be found that the graphene sheets predominantly distributed on the grain boundaries of aluminum matrix, and the distribution of graphene sheets in the composites is relatively homogeneous when the content of graphene sheets in the Al-Gr composites is up to 1.0 wt% (Fig .6 (a)-(c)). However, it is evident that the distribution of graphene sheets in the composite is not uniform and the aggregation of graphene sheets in the composite occurs in higher content of graphene sheets (Fig. 6 (d)). Bustamante et al. also reported that no clusters of graphene are observed in the reinforced composite with 1.0 wt% of graphene under the condition of ball milling [14].

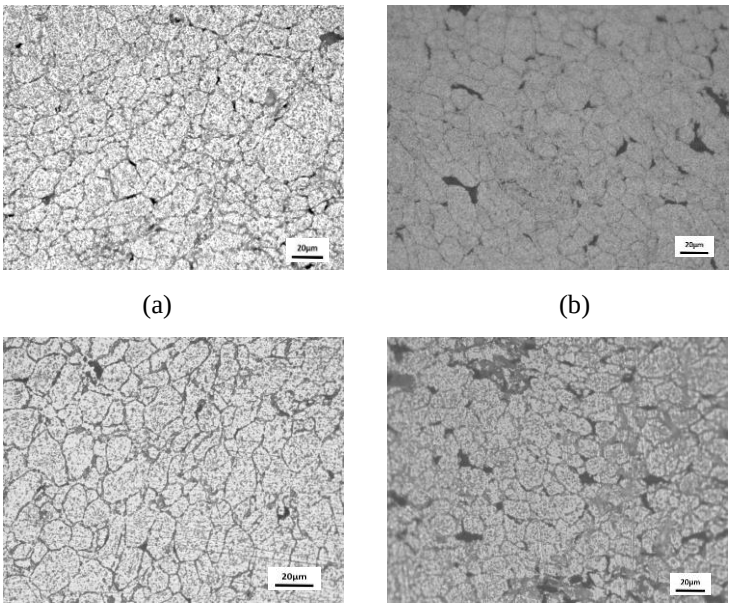


(a) (b)

(c) (d)

*Fig.6 Optical micrograph of hot-pressed Al-Gr composites:(a)0.3 wt.%, (b)0.7 wt.%, (c)1.0 wt.%, (d)1.2 wt.%*

Optical micrographs of Al-Gr composite as warm-rolled with graphene content of 0.3 wt.%, which was taken from different locations are shown in Fig. 7. It can be seen clearly that the crystal grains located at the surface is elongated along the rolling deformation direction, and there exists the fine grain zone of deformation. In the central position of the composite, no significant changes in grain size however were found. Rolling can also produce stress concentration, dislocation multiplication and densification of composite prepared by powder metallurgy. All these effects will strengthen the composite material. Graphene sheets are still distributed mainly along the grain boundaries. Compared with Fig. 6 (a), it's important to note that coordinated deformation of multilayer graphene sheets occurs with the deformation of the surface grains, which may cause a significant reduction in the number of layers of graphene sheets (Fig. 7(a)). It can be explained that the refinement of grain on the surface greatly increases the number of grain boundaries which can cause a reduction of thickness of the graphene sheets. For the central position of composite, there was no significant difference in the distribution of the graphene sheets on grain boundary before and after rolling (Fig. 6(a) and Fig. 7(b)).

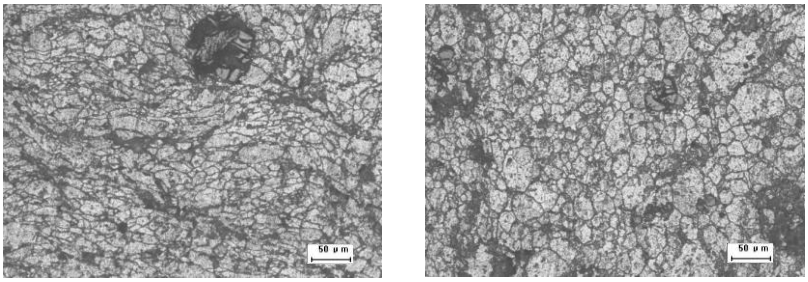


(a) (b)

*Fig.7 Optical micrograph of warm-rolled Al-0.3% Gr composite at different positions, (a) surface, (b) center.*

### 3.2 Density analysis and Vickers hardness

In order to determine the density of the warm-rolled composites the density of the composites was measured by the Archimedes method. Theoretical, experimental and relative densities of the various graphene content Al-Gr composites are shown in Fig. 8. It is found that the relative densities of the composites are more than 99%, which shows that the warm-rolled composites are dense, and the porosity of the composite is low. The relative density of the Al-Gr composites shows an decrease with increasing reinforcements (graphene sheets) contents (Fig. 8 (a)). This may be attributed to the low density (2.23g/cm$^3$) of graphene sheets. Fig. 8 (b) shows the variation of theoretical density and experimental density with variation of graphene content in the Al-Gr composites. The theoretical density decreases linearly with the addition of graphene sheets to the Al matrix. However, the experimental density is slightly lower than the theoretical density and also shows an decreases with the increase in the addition of graphene sheets up to 1.2 wt%. In addition, the increase in the amount of graphene sheets causes the poor combination among aluminum particles, which results in the increase of porosity in composites. It is also a major factor in the decline of the density.

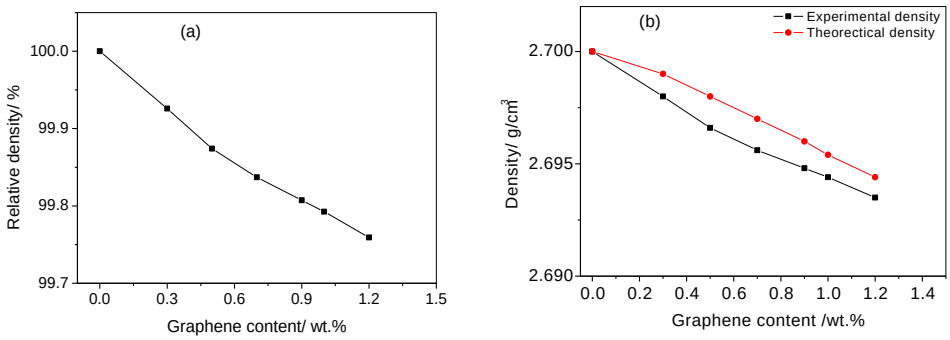


*Fig. 8. Variation of (a) relative density (b) theoretical density and experimental density of pure Al and the various Al-Gr composites.*

Vickers hardness values were measured for pure aluminum and it's warm-rolled composites. The measurements were repeated five times for each sample at random surface locations and averaged. The hardness results from the pure aluminium, the graphene sheets reinforced aluminium matrix composites samples are summarized in Fig. 9. With the increase of the content of graphene, the hardness of the composites increased and then decreased. The maximum of hardness is obtained at the graphene content of 0.7 wt.%. The hardness of the base material, pure aluminium sample, was 64.0±2.0 HV, while the hardness of 0.7 wt.% Gr-Al samples were 89.3 ± 3.2 HV, showing 39.5% increments over the unreinforced aluminium under otherwise identical experimental sample compaction and sintering conditions.

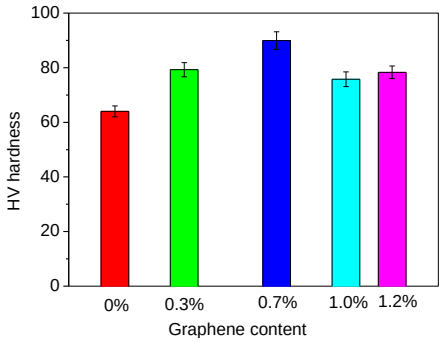


*Fig. 9. The Vickers hardness of the pure aluminium and various Gr/Al composites.*

### 3.3 Tribological characteristics

The variation in the measured coefficient of friction and wear rate with the weight percent of graphene in the composites (graphene content of 0.3, 0.7 and 1.2 wt.%) are shown in Fig. 10 (a) and (b). These results show that within the set of test conditions used, the coefficient of friction and wear rate in Al-Gr composites are significantly reduced compared with those in the matrix. It is clear from Fig. 10 (b) that even 0.3 wt.% of graphene addition can impose a significant reduction in the wear rate (by nearly on half) as compared with the un-reinforced alloy. The decreased coefficient of friction and wear rate of the Al-Gr composites with increased graphene content are generally expected from the self-lubricating composites. This conclusion is consistent

with that of Al-graphite composites reported by many investigators [14-17]. However, the report on the wear behavior of Al-graphene composites is scarce so far. We believe that the improved wear properties observed for the Al-graphene composites processed by the present method, can be attributed to the reasonably uniform distribution of graphene sheets within the fine grained matrix alloy.

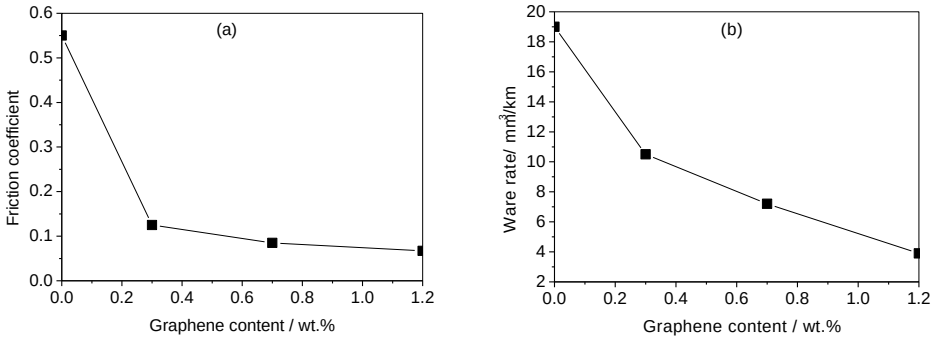


*Fig. 10. The effect of graphene addition on: (a) coefficient of friction; and (b) wear rate of composites.*

## 4. Conclusions

In this paper, the Al-Gr composites were fabricated by ball-milling mixing of pure aluminum powder and graphene sheets, followed by hot-pressing, sintering, and finally by rolling. The contents of graphene sheets were varied from 0.3 to 1.2 wt.% in aluminum matrix. The microstructures of as-sintered and as-rolled composites were analzsed, the density and hardness and wear property were tested for pure Al and Al–Gr composites in as-rolled states. Experimental results revealed that the graphene sheets are gradually dispersed into the aluminum matrix with increasing the ball-milling time and a uniform dispersion is achieved after ball-milling for 24 h. And no obvious agglomeration of graphene is observed in as-sintered and as-rolled composites for the contents of graphene sheets up to 1.0 wt.%.

The coordinated deformation of multilayer graphene sheets occurs with the deformation of the surface grains during rolling, which may cause a significant reduction in the number of layers of graphene sheets. With increasing the graphene sheets contents, The density of the Al-Gr composites shows an decrease. The maximal hardness of Al-Gr composites were 89.3 ± 3.2 HV at 0.7 wt.% of graphene content, showing 39.5% increments over pure aluminum. The coefficient of friction and wear rate in Al-Gr composites are significantly reduced compared with those in the matrix.

**Acknowledgements**

This work is supported by the Natural Science Foundation of Liaoning (201602642), the Research Foundation of Education Bureau of Liaoning Province, China (LG201620) and Shenyang Ligong University Key Laboratory Opening Fund in Advanced Materials Processing Technology in Liaoning Province, China.

## References


[1] K. S. Novoselov, A. K. Geim, S. V. Morozov, D. Jiang, Y. Zhang, S. V. Dubonos, I. V. Grigorieva, and A. A. Firsov, Science **306**, 666 (2004).

[2] A. K. Geim and K. S. Novoselov, Nat. Mater. **6**, 183 (2007).

[3] M. I. Katsnelson, Mater.Today **10**, 20 (2007).

[4] A. H. CastroNeto, F. Guinea, N. M. R. Peres, K. S. Novoselov, A. K. Geim, Rev. Mod. Phys. **81**, 109 (2009).

[5] M. Ishigami, J. H. Chen, W. G. Cullen, M. S. Fuhrer, E. D. Williams, NanoLett. **7**, 1643 (2007).

[6] J. Wu, W. Pisula, K. Müllen, Chem. Rev. **107**, 718 (2007).

[7] C. G. Lee, X. D. Wei, J. W. Kysar, J. Hone, Science **321**, 385 (2008).

[8] G. H. Lee, J. Hone, Science **340**, 1073 (2013).

[9] J. J. Liang, Y. Huang, L. Zhang, Y. S. Chen, Adv. Funct. Mater.**19**, 2297 (2009).

[10] J. Liu, H. X. Yan, K. Jiang, Cerm. Int. **39**, 6215 (2013).

[11] W. S. Hummers, R.Offeman, J. Am. Chem. Soc. **80**, 13 (1958).

[12] Y. Q. Qian, A. Vu, W. Smyrl, A. Stein, J. Electrochem. Soc. **159**, 1135 (2012).

[13] C. Suryanarayana, E. Ivanov, V. V. Boldyrev, Mater. Sci. Eng. **A 304-306**, 151 (2001).

[14] R. Pérez-Bustamante, D. Bolaons-Morales, J. Bonilla-Martínez, I. Estrada-Guel, R. Martínez-Sánchez, J. Alloys Compd. **615**, S578 (2014).

[14] P. K. Rohatgi, S. Ray, Y. Liu, Int. Mater. Rev. **37**, 129 (1992).

[15] Y. B. Liu, S. C. Lim, S. Ray, P. K. Rohatgi, Wear **159**, 201 (1992).

[16] H. Hocheng, S. B. Yen, T. Ishihara, B. K. Yen, Compos. A **28A**, 883 (1997).

[17] S. Das, S. V. Prasad, T. R. Ramachandran, Mater. Sci. Eng. **138A**, 123 (1991).